Staging of Untreated Squamous Cell Carcinoma of Buccal Mucosa with ^{18}F-FDG PET: Comparison with Head and Neck CT/MRI and Histopathology

Tzu-Chen Yen, MD, PhD[1,2]; Joseph Tung-Chieh Chang, MD, MHA[2,3]; Shu-Hang Ng, MD[2,4]; Yu-Chen Chang, MD[1,2]; Sheng-Chieh Chan, MD[1,2]; Hung-Ming Wang, MD[2,5]; Lai-Chu See, PhD[2,6]; Tsung-Ming Chen, MD[2,7]; Chung-Jan Kang, MD[2,7]; Yi-Fen Wu, BS[1,2]; Kun-Ju Lin, MD, PhD[1,2]; and Chun-Ta Liao, MD[2,7]

[1]Department of Nuclear Medicine, Chang Gung Memorial Hospital Linkou Medical Center, Taoyuan, Taiwan; [2]Taipei Chang Gung Head & Neck Oncology Group, Chang Gung Memorial Hospital Linkou Medical Center, Taoyuan, Taiwan; [3]Department of Radiation Oncology, Chang Gung Memorial Hospital Linkou Medical Center, Taoyuan, Taiwan; [4]Department of Diagnostic Radiology, Chang Gung Memorial Hospital Linkou Medical Center, Taoyuan, Taiwan; [5]Department of Hema-Oncology, Chang Gung Memorial Hospital Linkou Medical Center, Taoyuan, Taiwan; [6]Biostatistics Consulting Center/Department of Public Health, Chang Gung University, Taoyuan, Taiwan; and [7]Department of Otorhinolaryngology, Head and Neck Surgery, Chang Gung Memorial Hospital Linkou Medical Center, Taoyuan, Taiwan

This prospective, nonrandomized, case-control study evaluated the impact of ^{18}F-FDG PET in staging untreated squamous cell carcinoma of the buccal mucosa (BSCC) and compared the results with CT/MRI and histopathology. **Methods:** Between January 2002 and April 2004, 102 untreated BSCC patients with cM0 (no evidence of distant metastatic focus on chest radiograph, liver ultrasonograph, and bone scan) were enrolled with either conventional work-up (CWU, $n = 51$) or PET (CWU+PET, $n = 51$). All were monitored for at least 6 mo. The comparative diagnostic efficacies of PET and CT/MRI were evaluated using the area under the receiver-operating-characteristic curve (AUC). The primary endpoint was the percentage reduction in futile surgery (preoperative detection of distant metastatic lesions). The secondary endpoint was the 2-y cumulative recurrence rate among study participants (with PET) compared with that of comparable control subjects (without PET). **Results:** Significant benefits of PET compared with those of CT/MRI for BSCC patients were in the detection of locoregional (AUC, 0.973 vs. 0.928; $P = 0.026$), regional (AUC, 0.939 vs. 0.837; $P = 0.026$), and level II (AUC, 0.974 vs. 0.717; $P = 0.02$) lymph nodes. Two percent (1/51) of the patients experienced a reduction in futile surgery in the CWU+PET group compared with 0% (0/51) in the CWU group. However, no statistical difference was found in the 2-y locoregional control rate between the CWU and the CWU+PET groups. **Conclusion:** The role of ^{18}F-FDG PET for BSCC with cM0 is limited. Although PET is superior to CT/MRI in identifying cervical nodal metastases, it does not improve locoregional recurrence.

Received Oct. 7, 2004; revision accepted Jan. 16, 2005.

For correspondence or reprints contact: Chun-Ta Liao, MD, Department of Otorhinolaryngology, Chang Gung Memorial Hospital Linkou Medical Center, 5 Fu-Shin St., Kueishan, Taoyuan 333, Taiwan.

E-mail: liaoct@adm.cgmh.org.tw

Key Words: PET; ^{18}F-FDG; squamous cell carcinoma; buccal mucosa; staging

J Nucl Med 2005; 46:775–781

Asian and Western populations have their own characteristic disease spectra and cancer incidence. Thus, these populations may have divergence and disparities in their cancer pattern and priority of resource allocation. For example, squamous cell carcinoma of the buccal mucosa (BSCC), an aggressive oral cancer, is much more prevalent in Central and Southeast Asia than in Europe and the United States, where its occurrence is tied to the practice of betel quid chewing and tobacco smoking (*1,2*). In Western societies, the 5-y overall survival rates for patients with primary untreated BSCC is around 60% for cN0 and <50% for cN1–cN2, despite significant medical and surgical advances over the same period (*3,4*). This rate is <22% for those with local or nodal recurrence, despite salvage therapy (*3*).

In Taiwan, even with the assistance provided by free-flap reconstructions, tumor and nodal status are still the important independent risk factors of overall survival and locoregional relapse-free survival for BSCC. To date, surgery is the mainstay of the primary treatment mode for BSCC in Taiwan. Accurate preoperative staging of the disease is very important for surgical planning. In the past, CT and MRI were the standards used for staging BSCC. These conventional images relied on certain criteria, such as the nodal size and contrast-enhancement pattern. Though displaying a high sensitivity due to their

high spatial resolution, the techniques suffer from low specificities of detection of nodal metastases for various head and neck cancers (39% for CT and 48% for MRI) (*5–7*). The need for a more accurate preoperative staging for BSCC patients is pressing.

^{18}F-FDG PET has entered a new phase of development since a major technologic breakthrough in recent 10 y. Its application in head and neck cancer has become one of the standard imaging modalities in staging, restaging, treatment planning, and monitoring of therapeutic efficacy (*8–14*). With the additional help from PET, futile surgery can be reduced in 6%–17% of head and neck cancer patients (*15–17*). However, to our knowledge, there has not been a prospective study to date addressing the impact of ^{18}F-FDG PET on untreated BSCC patients. BSCC is an endemic cancer in Taiwan, with >100 untreated BSCC patients per year in our hospital alone. Therefore, we conducted this prospective study to understand the role of ^{18}F-FDG PET in the preoperative assessment of BSCC patients in a single-institute hospital. In this study, we focused on the clinical benefits of ^{18}F-FDG PET in reducing futile surgery as well as on improving locoregional recurrent control for BSCC patients.

MATERIALS AND METHODS

Patients and Study Design

This prospective, nonrandomized, case-control study was approved by the institutional review board of the Chang Gung Memorial Hospital (Taoyuan, Taiwan). Informed consent was obtained from each enrolled patient. Between January 2002 and April 2004, patients were divided into a conventional work-up group (CWU) or a PET group (CWU+PET). Eligibility criteria for CWU were a previously untreated BSCC with cM0, no contraindications to and a willingness to undergo contrast-enhanced CT/MRI, an unwillingness to pay for PET, and the presence of a potentially curable disease for which curative intent surgery was approved. Eligibility criteria for CWU+PET were a previously untreated BSCC with cM0, no contraindications to and a willingness to undergo contrast-enhanced CT/MRI and PET, a willingness to pay for PET, and the presence of a potentially curable disease and willingness to receive curative intent surgery. Patients were ineligible if they already had distant metastasis before primary treatment, were medically or psychologically unfit to receive curative intent surgical therapy, or had a history of other malignancy, excluding basal cell carcinoma of the skin. Potentially curable disease was defined as untreated BSCC without definite evidence of distant metastasis.

As patients were being assessed for their eligibility, panendoscopy, chest radiography, liver ultrasonography, whole-body bone scanning, and head and neck CT/MRI scanning were performed. cM0 was defined as no evidence of distant metastatic focus on chest radiograph, liver ultrasonograph, and bone scan. All subsequently enrolled patients underwent a whole-body ^{18}F-FDG PET scan. All examinations were performed within 2 wk. The clinical and pathologic staging was according to the 1997 criteria of the American Joint Committee on Cancer. The average diameter of the primary tumor was calculated from clinical inspection and results of the head and neck CT/MRI. Histopathologic results were taken as the gold standard of diagnostic accuracy for CT/MRI and PET.

CT/MRI Scan

CT was performed with the patient in the supine position with contrast axial scans. Images were parallel to the ramus of the mandible, from the skull base to the supraclavicular fossa with a 5-mm-thick contiguous section. A contrast coronal scan with a 3-mm-thick contiguous section was also obtained. In addition to the soft-tissue window settings, we reconstructed all images with bone algorithms. Patients underwent MRI with a 1.5-T unit (Vision; Siemens) using the spin-echo technique before and after injection of gadolinium diethylenetriaminepentaacetic acid (DTPA). A head coil was applied to examine the region from the superior margin of the temporal lobe to the level of the hyoid bone. A neck coil was used to examine the rest of the neck and the supraclavicular fossa. Unenhanced T1-weighted images were acquired in the sagittal and axial planes with a spin-echo 500/20 (repetition time/echo time, in ms) sequence with a 20-cm field of view and a 192 × 256 matrix. Axial and coronal T2-weighted, fat-suppressed fast-spin-echo images (3,000/85 [effective], 16 echo train length) were also obtained with 5 mm without an interslice gap in the axial projection and 4 mm without an interslice gap in the sagittal and coronal projections. After gadolinium DTPA injection (0.1 mmol/kg of body weight), we obtained T1-weighted, fat-suppressed axial, sagittal, and coronal sequences sequentially, with parameters similar to those used before gadolinium DTPA injection.

PET

The ^{18}F-FDG used in the PET scans was produced by the Institute of Nuclear Energy Research of Taiwan. All PET scans were acquired with a dedicated PET system (ECAT EXACT HR+ PET camera; Siemens/CTI) using a full width at half maximum of 4.5 mm and a transaxial field of view of 15 cm. All patients fasted for at least 6 h before PET. Diazepam (2 mg) was given before the injection of ^{18}F-FDG to reduce muscle uptake. After intravenous injection of 370 MBq (10 mCi) of ^{18}F-FDG, patients were kept at rest in a quiet, dimly lit room for at least 40 min. Talking, walking, and other physical activities were avoided to reduce muscle uptake. Dual-phase PET was performed while patients were in the supine position and along the central axis of the PET table. Initially, seven 2-dimensional mode, sequential images, including a 5-min emission scan and a 3-min transmission scan for each bed position, from the head to the upper thigh were obtained over a 56-min period. After 3 h, the second-phase PET scan was performed from the neck to the head for another 3 fields of view with the same emission and transmission acquisition time. This required a further 24 min. Transmission scans was performed by three ^{68}Ge/^{68}Ga rod sources to obtain attenuation corrections. Reconstruction of transmission and emission scans used accelerated maximum likelihood reconstruction. Maximum-intensity-projection images were viewed on a workstation that allowed simultaneous viewing of coronal, sagittal, and transverse planes as well as a 3-dimensional rotation projection. The anatomic reference for whole-body PET was the apex of the heart, circumference of the liver, kidney, urinary bladder, and the bone marrow of the vertebral column. The standardized uptake value (SUV) was obtained by analysis of the region of interest (ROI). The ROI was placed on the emission image at the area of increased ^{18}F-FDG uptake. The location of the edge of the ROI was the contour for 75% of the peak counts.

Image Interpretation and Analysis

Two radiologists interpreted CT/MRI studies without knowledge of the PET findings. Three experienced nuclear medicine physicians who were unaware of the MRI findings interpreted the PET studies individually by visual inspection of transverse, sagittal, and coronal section scans. The SUV of the ^{18}F-FDG uptake was used as an accessory reference. Based on the intensity and the anatomic region of the uptake, any uptake more than normally interpreted as physiologic was identified and then scored on a 5-point scale: 0 = no abnormal uptake, 1 = benign, 2 = probably benign, 3 = probably malignant, and 4 = definitely malignant (*18*). A checklist of the distributions of tumor extension, nodal spread, and distant metastasis was recorded accordingly. Grades 3 and 4 were considered to be positive results. Any initial difference of opinion was solved by consensus.

Outcome Determination and Data Analysis

Results of PET, CT/MRI, and clinical examinations were discussed jointly by the head and neck research team, consisting of the nuclear medicine physicians, head and neck radiologists, head and neck surgical oncologists, medical oncologists, and radiation oncologists. To determinate whether there were unexpected contralateral cervical malignant nodes or distant metastasis on the basis of the combined reading of PET and CT/MRI, we also recorded the same checklist together and resolved any discordance by consensus. Relevant information was obtained from a thorough review of all relevant records and discussion among the members of the research team. Postoperative histologic examination of primary tumors and lymph nodes in the neck dissection specimens provided the diagnostic gold standard. The neck dissection specimens were labeled precisely by the surgeon according to the neck levels dependent on the imaging-based nodal classification used in the interpretation of PET and CT/MRI. On the basis of the histologic findings, PET results were classified as true-positive, true-negative, false-positive, or false-negative. To assess the efficacy of PET to conventional images, we compared the area under the curve (AUC) between those with head-and-neck CT/MRI only and those with CT/MRI plus whole-body PET.

Adjuvant Treatment

According to the consensus and treatment guideline for the head and neck oncology group, adjuvant radiotherapy (RT) was delivered to the patients with pathologically stage T4 or N1 without node extracapsular spreading (ECS) or to those patients with close resection margins (<5 mm). Concomitant chemoradiotherapy was prescribed for the patients with node extracapsular spreading, >1 node metastasis, or positive resection margins. The radiation treatment portal included the primary tumor bed with general margins and the 1–2 levels beyond pathologically positive neck nodes above the clavicle for 46–50 Gy and then decreased the RT field to include the tumor bed with close margins and a pathologically positive node area to total 60–66 Gy. The radiation was delivered at 2 Gy per fraction and 5 fractions per week and by a 3-dimensional conformal radiation technique. The chemotherapy given was cisplatin-based regimens administered every 1 to 2 wk during RT in the outpatient clinic.

Clinical Characteristics of Study Participants and Comparable Control Subjects

Information prospectively recorded for both comparable and study cohorts included age at initial diagnosis, sex, histologic type and grade of differentiation at initial diagnosis, TNM stage, type of primary treatment, adjuvant therapy use, results of all biopsies, pattern of recurrence, evidence (histologic, radiographic, or clinical) and site(s) of disease progression after salvage therapy, and status (alive or dead, with or without recurrence) at the date of the last follow-up. PET results, including the SUV and the visual score for each site, and information on the treatment plan before and after PET were recorded prospectively for the study cohort.

Statistical Analysis

The study was a safety and efficacy open-labeled trial. The primary endpoint was the percentage reduction of futile surgeries (to detect distant metastatic lesion(s) preoperatively). The secondary endpoint was the relative benefit in terms of a 2-y cumulative recurrence rate between study patients (with PET) and comparable control subjects (without PET). At the time of the protocol design, toxicity related to guided biopsy or curative intent surgery was to be measured using the National Cancer Institute Common Toxicity Criteria for Adverse Events version 3.022. A visual score of 3 or 4 was considered to be positive in calculations of sensitivity, specificity, and accuracy, and scores of 0–2 were considered to be negative. The AUC using the receiver-operating-characteristic (ROC) curve was used to calculate the additional benefit of PET to MRI (*19*). When applicable, the χ^2 test was used to examine differences in clinical covariates between groups. Recurrent-free survival curves were plotted according to the Kaplan–Meier method and the log-rank test was used to evaluate the significance of the differences between the curves (*20*). All *P* values presented are 2-sided.

RESULTS

Patient Characteristics

The flow chart of the study is presented in Figure 1. Between January 2002 and April 2004, 114 consecutive untreated BSCC patients with cM0 planning to have surgical treatment were enrolled. Fifty-eight patients were assigned to the CWU group and 56 were assigned to the CWU+PET group. Seven patients were subsequently excluded from the CWU group due to incomplete MRI data (n = 4) or their loss during follow-up (n = 3). In the CWU+PET group, 5 patients were excluded due to incomplete MRI data (n = 4) or their loss during follow-up (n = 1). The resulting study population was 102 untreated BSCC patients (51 for CWU and 51 for CWU+PET).

The enrolled patients were further divided according to their clinical stage of disease progression, since early stages (I and II) are highly curable and treatable by surgery or RT alone with late stages (III and IV) having a relatively poor prognosis, with treatment typically comprised of surgery followed by RT or concurrent chemoradiation therapy (*21–23*). The characteristics of the study group (n = 51) and the comparable group (n = 51) are listed in Table 1. We performed neck dissection in almost all patients. The neck dissection area was determined by clinical and image findings. Usually we performed supraomohyoid neck dissection in clinically negative and image-negative neck patients and modified neck dissection in positive neck node patients. Forty-nine patients with PET received neck dissection; among them, the extension of the neck dissection field was

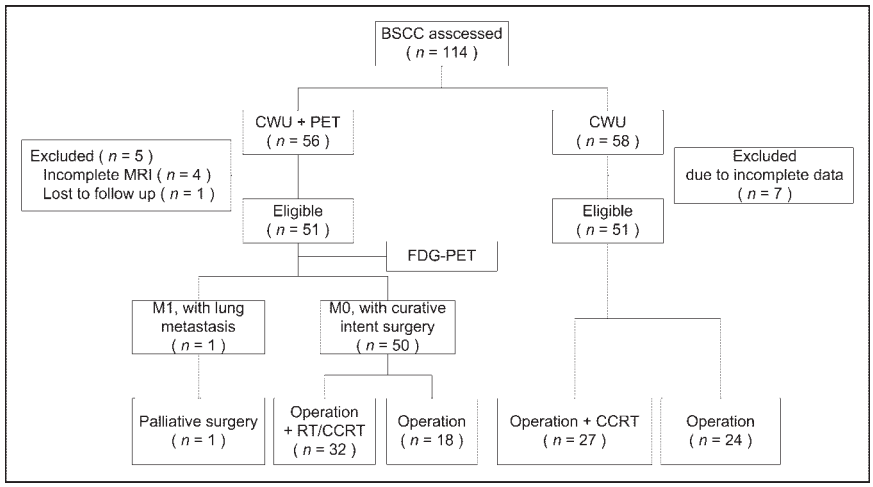

FIGURE 1. Trial profile. CCRT = concurrent chemotherapy and radiation therapy.

changed in 3 patients because PET findings suggested level IV nodal metastases in 2 patients and contralateral nodal metastases in the other one. However, these PET findings proved to be pathologically negative. No significant differences between the age at initial diagnosis, sex, histology, TNM stage, and mode of primary treatment were evident. All patients were monitored for at least 6 mo, with a median follow-up time of 16.5 mo.

TABLE 1
Clinical Characteristics of BSCC Patients: Those With (n = 51) and Without (n = 51) PET

Clinical characteristic	PET		P
	With	Without	
Age (y)			
≤40	5 (10)	9 (18)	0.389
>40	46 (90)	42 (82)	
Sex			
M	49 (96)	50 (98)	1.000
F	2 (4)	1 (2)	
Cell type			
WD SCC + MD SCC	48 (94)	44 (86)	0.318
PD SCC	3 (6)	7 (14)	
AJCC c-stage			
I–II	15 (29)	16 (31)	1.000
III–IV	36 (71)	35 (69)	
AJCC p-stage			
I–II	14 (27)	16 (31)	0.661
III–IV	37 (73)	35 (69)	
Mode of primary treatment			
With free-flap reconstruction	46 (90)	48 (94)	0.715
Without free-flap reconstruction	5 (10)	3 (6)	
With neck dissection	49 (96)	46 (90)	0.436
Without neck dissection	2 (4)	5 (10)	
Surgery	19 (37)	24 (49)	0.230
Surgery + RT/CCRT	32 (63)	27 (51)	

WD = well differentiated; SCC = squamous cell carcinoma; MD = moderately differentiated; PD = poorly differentiated; AJCC = American Joint Committee on Cancer; c-stage = clinical stage; p-stage = pathologic stage; CCRT = concurrent chemoradiation therapy.

Data are expressed as number (%) with and without PET.

Diagnostic Benefit of ^{18}F-FDG PET Compared with CT/MRI

Figure 2 depicts the nodal metastatic pattern in the 51 CWU+PET patients. Our results demonstrated that either CT/MRI alone or combined PET and CT/MRI detected all primary tumors. Twenty-five patients (49%) had nodal metastases and 26 were N0. Level I was the most common site for nodal metastases (25/25, 100%), followed by level II

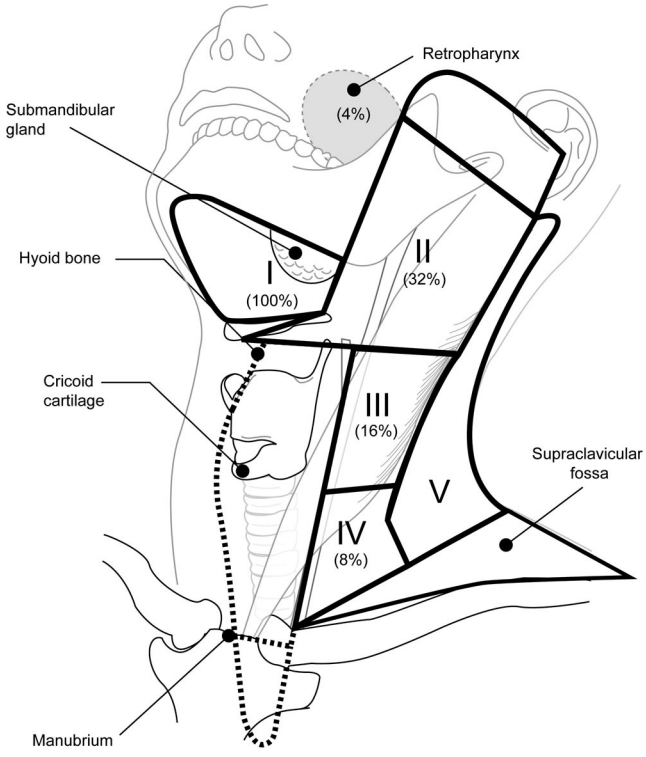

FIGURE 2. Distribution of lymphadenopathy in 51 BSCC patients with nodal metastasis.

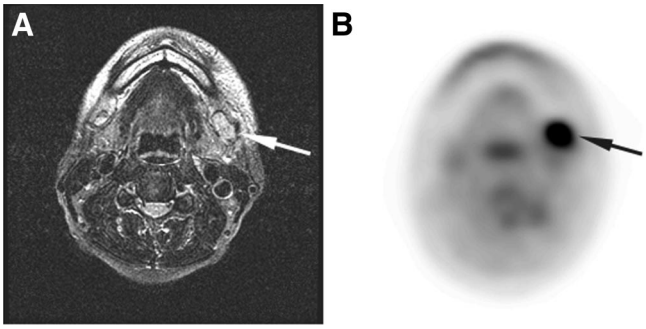

FIGURE 3. A 52-y-old patient with left buccal cancer, T3 N2b M0. (A) Transaxial T2-weighted MR image reveals enlarged neck lymph node at left level IB (arrow). (B) Transaxial ^{18}F-FDG PET image shows ^{18}F-FDG–avid lesion at same level (arrow). Subsequent nodal dissection showed a metastatic node at level IB.

(8/25, 32%), level III (4/25, 16%), level IV (2/25, 8%), and a retropharyngeal lymph node (1/25, 4%). Only 1 patient (4%) displayed nodal metastases to both ipisilateral and contralateral sites at level II. According to the histopathologic examinations, 5 nodes were missed by CWU+PET. Two were at level I, 1 was at level II, 1 was at level III, and 1 was at level IV. All were intranodal tumor deposits, ranging from 2 to 6 mm. In addition, 9 nodes were false-negative on CT/MRI but true-positive on PET (1 was at a retropharyngeal lymph node, 4 were at level I, 2 were at level II, 1 was at level III, and 1 was at level IV) and 1 node was true-positive on CT/MRI but false-negative on PET (level I).

A benefit of an imaging method means identification of tumor involvement at the primary site or of a lymph node. In this study, we found a significant benefit of the combination of ^{18}F-FDG PET and CT/MRI over head and neck CT/MRI alone for BSCC patients in the overall assessment of the primary sites and the neck (AUC, 0.973 vs. 0.928; $P = 0.026$) as well as in assessing the regional nodes (AUC, 0.939 vs. 0.837; $P = 0.026$) and the level II nodes (AUC, 0.974 vs. 0.717; $P = 0.02$). However, the combination of ^{18}F-FDG PET and CT/MRI did not significantly increase the sensitivity and specificity of CT/MRI in level I (88% vs. 76%, $P = 0.375$; 92% vs. 81%, $P = 0.25$) (Figs. 3 and 4) and the sensitivity in level III (75% vs. 50%, $P = 1.0$; 98% vs. 98%, $P = 1.0$) (Table 2).

Benefits of PET for BSCC Staging

Ten BSCC patients had locoregional recurrence. Of these, 6 were in the CWU+PET group and 4 were in the CWU group. Seventeen of the total number of BSCC patients had distant metastases at the time of the last follow-up. Of these, 7 were in the CWU+PET group and 10 were in the CWU group. In the CWU+PET group, only 1 patient was observed to have distant metastasis (lung) preoperatively by use of PET. There was no significant difference of the 2-y locoregional control between the CWU+PET group (86%) and the CWU group (87%) ($P = 0.4421$) (Fig. 5).

DISCUSSION

BSCC is an endemic carcinoma in regions of Central and Southeast Asia, including Taiwan. Both metastatic status (M0 vs. M1) and nodal status (N0 vs. N+) strongly influence the survival in BSCC patients and prelude a comparatively worse prognosis (*3,24,25*). When distant metastasis is detected preoperatively, appropriate palliation instead of primary tumor excision or neck dissection is indicated. Therefore, a decision regarding curative or palliative treatment is crucial for untreated BSCC patients.

^{18}F-FDG PET has potential in decreasing unnecessary surgery in cases of head and neck cancer where lesions have already metastasized (*15–17*). Distant metastases or secondary tumors can be found in 9%–12% of European patients with an average age of >60 y (*15*). Given that the tumor biology of BSCC in Asia may be different from that of European patients for different etiologies and different age groups (*26*), we were interested in evaluating the potential of ^{18}F-FDG PET for BSCC patients with cM0. In the present prospective study, 7 (14%) BSCC patients in the CWU+PET group had distant metastasis at the time of their last follow-up. Of these, only 1 patient was found to have lung metastases by PET preoperatively. The low rate of preoperative PET detection may have been due to the undetectably small size of the distant metastatic lesions. Alternately, distant metastasis may not have been present initially, with dissemination occurring coincident with the surgery or secondarily to local or locoregional recurrence. In the CWU+PET group, 29% (2/7) patients already had local ($n = 1$) or locoregional ($n = 1$) recurrence before their distant metastases. This implies that the contribution of PET for the early detection of distant metastatic lesions for BSCC patients might be limited.

For nodal status, BSCC is believed to occur less frequently than that for other oral cavity cancers with an incidence of 16%–28% (*3,27,28*), although the incidence

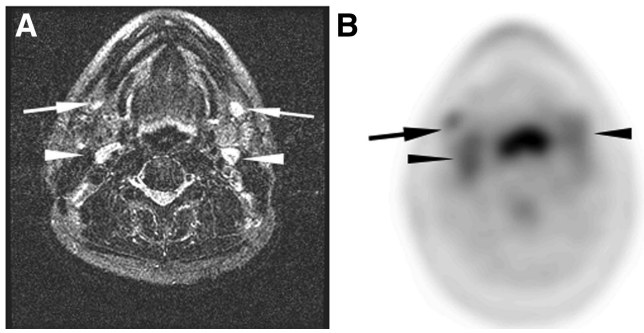

FIGURE 4. A 51-y-old man who presented with left buccal cancer, T2 N0 M0. (A) Transaxial T2-weighted MR image reveals 2 benign neck lymph nodes at bilateral level IB (arrows). Two equivocal neck nodes are also noted, posterior to submandibular glands of level II (arrowheads). (B) Corresponding ^{18}F-FDG PET image at same level reveals faintly ^{18}F-FDG–avid lesions (arrow and arrowheads), which supported neck nodes being benign. Histopathologic examination was negative after neck dissection. He was well 1 y after surgery.

TABLE 2
Results of ^{18}F-FDG PET on 51 BSCC Patients in Head and Neck Region

Site	FN (*n*)	TP (*n*)	TN (*n*)	FP (*n*)	Sensitivity %	Sensitivity 95% CI (%)	Specificity %	Specificity 95% CI (%)	Accuracy %	Accuracy 95% CI (%)	AUC	*P*
Main												
CT/MRI	0	51	0	0	100		—		100			
^{18}F-FDG PET + CT/MRI	0	51	0	0	100		—		100			
Retropharyngeal LN												0.089
CT/MRI	1	0	50	0	0		100		98	90–100	0.500	
^{18}F-FDG PET + CT/MRI	0	1	50	0	—		100		100		1	
Level I LN												0.290
CT/MRI	6	19	21	5	76	55–91	81	61–93	78	65–89	0.853	
^{18}F-FDG PET + CT/MRI	3	22	24	2	88	69–98	92	75–99	90	79–97	0.915	
Level II LN												0.020
CT/MRI	4	4	38	5	50	16–84	88	75–96	82	69–92	0.717	
^{18}F-FDG PET + CT/MRI	1	7	39	4	88	47–100	91	78–97	90	79–97	0.974	
Level III LN												0.110
CT/MRI	2	2	46	1	50	7–93	98	89–100	94	84–99	0.729	
^{18}F-FDG PET + CT/MRI	1	3	46	1	75	19–99	98	89–100	96	87–100	0.981	
Level IV LN												0.440
CT/MRI	2	0	49	0	0		100		96	87–100	0.490	
^{18}F-FDG PET + CT/MRI	1	1	49	0	50	1–99	100		98	90–100	0.730	
Level V LN												
CT/MRI	0	0	50	1	—		98	90–100	98	90–100		
^{18}F-FDG PET + CT/MRI	0	0	51	0	—		100		100			
Total LN												0.026
CT/MRI	15	25	254	12	63	46–77	96	92–98	91	87–94	0.837	
^{18}F-FDG PET + CT/MRI	6	34	259	7	85	70–94	97	95–99	96	93–98	0.939	
Total lesions												0.026
CT/MRI	15	76	254	12	84	74–91	96	92–98	92	89–95	0.928	
^{18}F-FDG PET + CT/MRI	6	85	259	7	93	86–98	97	95–99	96	94–98	0.973	

FN = false-negative; TP = true-positive; TN = true-negative; FP = false-positive; CI = confidence interval; LN = lymph node.

may be up to 50% in people <35 y old (*29*). In contrast, we observed an incidence of cervical nodal metastases for BSCC patients of 49%, with most of these cases involving patients >35 y old. This result implies that even with the same histopathology, a different tumor biology is manifest in characteristic and variant disease spectra and cancer patterns. The presently observed incidence of nodal metastases was higher in our Taiwanese patients than that found in Indian patients (*22*), despite similar pathology in the 2 populations. It is conceivable that with similar etiologies, differences in tumor biology exist (*26*).

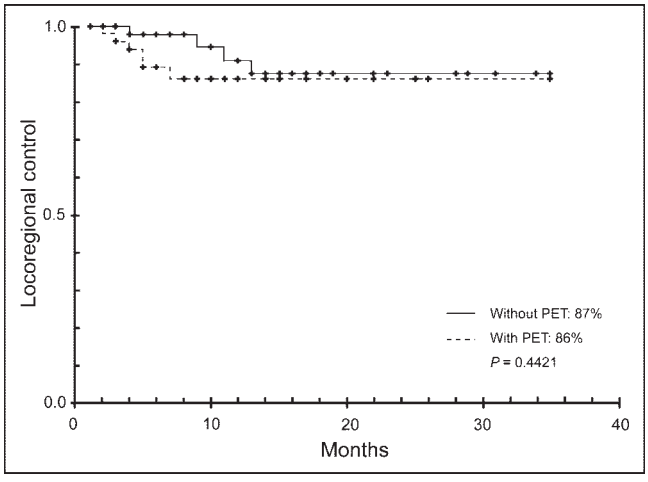

FIGURE 5. Kaplan–Meier plots of locoregional control according to PET use for untreated BSCC.

^{18}F-FDG PET is helpful to CWU in the primary staging of head and neck cancer patients (*8,9*). Considering the different tumor biology of BSCC from other head and neck cancers, we sought to further understand the potential benefit of ^{18}F-FDG PET to CWU in BSCC. Our results demonstrate that either CT/MRI or combined PET and CT/MRI can detect all primary tumors. However, in the detection of metastatic lesions to cervical nodes, 15% of the node lesions were missed using PET and CT/MRI. Careful analysis of these false-negative nodes revealed that, although all had high glucose transporter I expression, the tumor size (2–6 mm) may well have been too small to be detected by PET. Moreover, once cervical nodal metastasis occurred, level I was the most common site. Thus, detection of the cervical nodal form by either MRI or PET/CT should warrant examination of level I nodes.

Locoregional recurrence is a serious issue for BSCC. In our experience, most recurrent tumors are advanced and unresectable. Therefore, locoregional failure becomes the major cause of death for BSCC patients. ^{18}F-FDG PET is useful for primary head and neck cancer patients in treatment planning (*8,9*). The impact of ^{18}F-FDG PET in locoregional control of BSCC is poorly defined. In our histologic records, although the 5-y overall survival for treated BSCC patients is relatively high (68%), the 3-y overall survival for those with either recurrence at local or nodal sites is lower (30%), even with salvage therapy. Presently, we have found that ^{18}F-FDG PET is of no benefit in improving local or locoregional control compared with that of the comparable control group. There are 2 possible reasons. First, >90% of the BSCC patients in our group had free-flap–based reconstruction for radical tumor excision. Second, 96% of our BSCC patients had neck dissection. In the present study, 93.3% (14/15) of false-negative nodes, either on CT/MRI or PET, were at the neck region (level I to level IV) and could be removed by neck dissection. The other node at the retropharyngeal region could be removed by radical tumor dissection. Therefore, in this study, the curative treatment planning (a contralateral neck lymph node metastases identified by PET) was changed for only 6% (3/49) of the patients.

CONCLUSION

In comparison with comparable control subjects, ^{18}F-FDG PET has a limited contribution in avoiding futile surgery. Although ^{18}F-FDG PET improves the capability of CT/MRI in identifying cervical nodal metastases, ^{18}F-FDG PET does not improve locoregional recurrence in BSCC patients.

ACKNOWLEDGMENT

This work was supported by grants from Chang Gung Memorial Hospital (CMRPG-32034 and CMRPG-32039).

REFERENCES

1. Chen YK, Huang HC, Lin LM, Lin CC. Primary oral squamous cell carcinoma: an analysis of 703 cases in southern Taiwan. *Oral Oncol.* 1999;35:173–179.
2. Vegers JW, Snow GB, van der Waal I. Squamous cell carcinoma of the buccal mucosa: a review of 85 cases. *Arch Otolaryngol.* 1979;105:192–195.
3. Diaz EM Jr, Holsinger C, Zuniga ER, Robert DB, Sorensen DM. Squamous cell carcinoma of the buccal mucosa: one institution's experience with 119 previously untreated patients. *Head Neck.* 2003;25:267–273.
4. Brown AE, Langdon JD. Management of oral cancer. *Ann R Coll Surg Engl.* 1995;77:404–408.
5. Curtin H, Ishwararn H, Mancuso H, Dalley B, Caudry D, McNeil B. Comparison of CT and MRI imaging in staging of neck metastases. *Radiology.* 1998;207:123–130.
6. Lell M, Baum U, Greess H, et al. Head and neck tumors: imaging recurrent tumor and post-therapeutic changes with CT and MRI. *Eur J Radiol.* 2000;33:239–247.
7. Popperl G, Lang S, Dagdelen O, et al. Correlation of FDG-PET and MRI/CT with histopathology in primary diagnosis, lymph node staging and diagnosis of recurrency of head and neck cancer. *Fortschr Geb Rontgenstr Bildgebenden V.* 2000;174:714–720.
8. Schwartx DL, Rajendran J, Yueh B, et al. Staging of head and neck squamous cell cancer with extended-field FDG-PET. *Arch Otolaryngol Head Neck Surg.* 2003;129:1173–1178.
9. Kresnik E, Mikosch P, Gallowitsch HJ, et al. Evaluation of head and neck cancer with ^{18}F-FDG PET: a comparison with conventional methods. *Eur J Nucl Med.* 2001;28:816–821.
10. Lowe VJ, Boyd JH, Dunphy FR, et al. Surveillance for recurrent head and neck cancer using positron emission tomography. *J Clin Oncol.* 2000;18:651–658.
11. Wong RF, Lin DT, Schöder H, et al. Diagnostic and prognostic value of [^{18}F]fluorodeoxyglucose positron emission tomography for recurrent head and neck squamous cell carcinoma. *J Clin Oncol.* 2002;20:4199–4208.
12. Halfpenny W, Hain SF, Biassoni L, Maisey MN, Sherman JA, McGurk M. FDG-PET: a possible prognostic factor in head and neck cancer. *Br J Cancer.* 2002;86:512–516.
13. Brun E, Kjellén E, Tennvall J, et al. FDG PET studies during treatment: prediction of therapy outcome in head and neck squamous cell carcinoma. *Head Neck.* 2002;24:127–135.
14. Scarfone C, Lavely WC, Cmelak AJ, et al. Prospective feasibility trial of radiotherapy target definition for head and neck cancer using 3-dimensional PET and CT imaging. *J Nucl Med.* 2004;45:543–552.
15. Goerres GW, Schmid DT, Gratz KW, van Schulthess GK, Eyrich GK. Impact of whole body positron emission tomography on initial staging and therapy in patients with squamous cell carcinoma of the oral cavity. *Oral Oncol.* 2003;39:547–551.
16. Kitagawa Y, Nishizawa S, Sano K, et al. Whole-body ^{18}F-fluorodeoxyglucose positron emission tomography in patients with head and neck cancer. *Oral Surg Oral Med.* 2002;93:202–207.
17. Teknos TN, Rosenthal EL, Lee D, Taylor R, Marn CS. Positron emission tomography in the evaluation of stage III and IV head and neck cancer. *Head Neck.* 2001;23:1056–1060.
18. Yen TC, Ng KK, Ma SY, et al. Value of dual-phase 2-fluoro-2-deoxy-d-glucose positron emission tomography in cervical cancer. *J Clin Oncol.* 2003;21:3651–3658.
19. Metz CE. ROC methodology in radiologic imaging. *Invest Radiol.* 1986;21:720–733.
20. Mantel N. Evaluation of survival data and two rank order statistics arising in its consideration. *Cancer Chemother Rep.* 1966;50:163–170.
21. Nair MK, Sankaranarayanan R, Padmanabhan TK. Evaluation of the role of radiotherapy in the management of carcinoma of the buccal mucosa. *Cancer.* 1988;61:1326–1331.
22. Mishra RC, Singh DN, Mishra TK. Post-operative radiotherapy in carcinoma of buccal mucosa, a prospective randomized trial. *Eur J Surg Oncol.* 1996;22:502–504.
23. Fang FM, Leung SW, Huang CC, et al. Combined-modality therapy for squamous carcinoma of the buccal mucosa: treatment results and prognostic factors. *Head Neck.* 1997;19:506–512.
24. Fleming ID, Cooper JS, Henson DE, et al. *AJCC Cancer Staging Manual.* 6th ed. Philadelphia, PA: Lippincott Williams & Wilkins; 2002:23–32.
25. Pop LA, Eijkenboom WM, de Boer MF, et al. Evaluation of treatment results of squamous cell carcinoma of the buccal mucosa. *Int J Radiat Oncol Biol Phys.* 1989;16:483–487.
26. Hsieh LL, Wang PF, Chen IH, et al. Characteristics of mutations in the p53 gene in oral squamous cell carcinoma associated with betel quid chewing and cigarette smoking in Taiwanese. *Carcinogenesis.* 2001;22:1497–1503.
27. Dhawan IK, Verma K, Khazanchi RK, Madan NC, Shukla NK, Saxena R. Carcinoma of buccal mucosa: incidence of regional lymph node involvement. *Indian J Cancer.* 1993;30:176–180.
28. Sieczka E, Datta R, Singh A, et al. Cancer of the buccal mucosa: are margins and T-stage accurate predictors of local control? *Am J Otolaryngol.* 2001;22:395–399.
29. Iype EM, Pandey M, Mathew A, Thomas G, Nair MK. Squamous cell cancer of the buccal mucosa in young adults. *Br J Oral Maxillofac Surg.* 2004;42:185–189.

The Journal of NUCLEAR MEDICINE

Staging of Untreated Squamous Cell Carcinoma of Buccal Mucosa with ^{18}F-FDG PET: Comparison with Head and Neck CT/MRI and Histopathology

Tzu-Chen Yen, Joseph Tung-Chieh Chang, Shu-Hang Ng, Yu-Chen Chang, Sheng-Chieh Chan, Hung-Ming Wang, Lai-Chu See, Tsung-Ming Chen, Chung-Jan Kang, Yi-Fen Wu, Kun-Ju Lin and Chun-Ta Liao

J Nucl Med. 2005;46:775-781.

The Journal of Nuclear Medicine is published monthly.
SNMMI | Society of Nuclear Medicine and Molecular Imaging
1850 Samuel Morse Drive, Reston, VA 20190.
(Print ISSN: 0161-5505, Online ISSN: 2159-662X)

SNMMI SOCIETY OF NUCLEAR MEDICINE AND MOLECULAR IMAGING